Title
Vehicle Traction Control And its Applications

Authors
Kachroo, Pushkin
Tomizuka, Masayoshi

Publication Date
1994

CALIFORNIA PATH PROGRAM
INSTITUTE OF TRANSPORTATION STUDIES
UNIVERSITY OF CALIFORNIA. BERKELEY

Vehicle Traction Control and Its Applications

Pushkin Kachroo
Masayoshi Tomizuka

California PATH Research Paper

UCB-ITS-PRR-94-08

This work was performed as part of the California PATH Program of the University of California, in cooperation with the State of California Business, Transportation, and Housing Agency, Department of Transportation; and the United States Department Transportation, Federal Highway Administration.

March 1994

ISSN 1055-1425

Vehicle Traction Control And Its Applications

Pushkin Kachroo and Masayoshi Tomizuka
Department of Mechanical Engineering
University of California at Berkeley
Berkeley, California 94720

Abstract

Control of vehicle traction is of utmost importance in providing safety and obtaining desired vehicle motion in longitudinal and lateral vehicle control. Vehicle traction control systems can be designed to satisfy various objectives of a single vehicle system or a platoon of vehicles in an automated highway system, which include assuring ride quality and passenger comfort. Other objectives are aimed at providing desirable longitudinal and lateral motion of the vehicles.

Vehicle traction force directly depends on the friction coefficient between road and tire, which in turn depends on the wheel slip as well as road conditions. From control point of view, we may influence traction force by varying the wheel slip. Wheel slip is a nonlinear function of the wheel velocity and the vehicle velocity. In this paper, a robust adaptive sliding mode controller is designed to maintain the wheel slip at any given value. Different objectives of traction control, give different target slips to be followed. Simulation study shows that longitudinal controllers, which do not take traction into account explicitly (termed as tractionless or passive controllers), cannot handle external disturbances well; on the other hand, longitudinal traction controllers (termed as active controllers) give satisfactory results with the same disturbances. Simulations show how some of the vehicle

performance objectives are met by using traction controllers.

1. Introduction

Vehicle traction control can greatly improve the performance of vehicle motion and stability by providing anti-skid braking and anti-spin acceleration. Vehicle traction control is especially important for automated highway systems as related to longitudinal and lateral control.

Many companies have developed and used anti-lock braking (ABS) and anti-slip acceleration control systems [7,11]. A typical commercial ABS system is composed of sensors, a control unit and a brake pressure modulator. In the prediction stage, the control logic of such a system uses information from the wheel angular velocity and/or acceleration to estimate the wheel slip. Wheel slip is a nonlinear function of wheel angular velocity and vehicle velocity and is described in more detail in section-2. The control command is based on the estimated slip and wheel acceleration. The wheel slip/acceleration phase plane is divided into different sectors. Each sector has a corresponding control action (e.g. APPLY, HOLD, RELEASE). This design process tries to produce an optimal limit cycle in the phase plane of wheel slip and acceleration. The control stage of the algorithm is usually referred to as the selection stage. Similar algorithms are designed for anti-spin acceleration. Although these systems work in practice, their design is experimental rather than analytical, and their tuning and calibration rely on trial and error. With the recent advances in sensor technology [2], controllers can be designed to maintain a specified wheel slip.

In the context of highway automation as it relates to the California Program on Advanced Technology for Highways (PATH), we can use an alternate method to estimate wheel slip. As angular wheel velocity is measured directly, we only need vehicle velocity to estimate slip. For lateral control of vehicles in the PATH program, magnetic markers are

installed on the road at specified distances from each other in the longitudinal directions. Vehicle velocity can thus be estimated by measuring the time elapsed between consecutive markers.

Another method to estimate the vehicle velocity would be to use an accelerometer. Accelerometers measure acceleration which can be integrated to calculate velocity. To avoid accumulation of integration error, the initial velocity should be updated (from wheel angular velocity) every few seconds before acceleration or braking starts. At the initiation of acceleration or braking, the last initial condition should be used for the integration process. Additional hardware may also be required to reduce the accumulation of the error due to the slope of the road.

In this paper, it is assumed that vehicle velocity and wheel angular velocity are both available on-line by direct measurements and/or estimations.

A controller for vehicle motion should address safety and stability of the vehicle. As a part of highway automation, longitudinal and lateral guidance of the vehicle should be addressed. The input forces, which control the vehicle motion come from the road-tire interaction and have two components, one in the longitudinal direction and one in the lateral direction. The tractive force in the lateral direction depends on the cornering stiffness and can be controlled by the steering [8, 9]. The tractive force in the longitudinal direction, on the other hand, is a nonlinear function of the wheel slip and can be controlled by maintaining the wheel slip at some required value. The throttle and the brakes ultimately control the longitudinal tractive force. Controlling the longitudinal traction can achieve various control objectives while assuring ride quality and passenger comfort. A few of these are:

(1) Maintain the fastest stable acceleration and deceleration.

(2) Obtain anti-skid braking and anti-spin acceleration.

(3) Maintain steer-ability during lateral maneuvers.

(4) Make vehicles move longitudinally in a platoon following the vehicles in front in

an automated highway system.

(5) Make a platoon of vehicles follow a desired lateral and longitudinal path simultaneously in an automated highway system.

A vehicle system could also use different traction control algorithms at different times after assessing which control law is appropriate at that time instant. A supervisory control could be devised to make such decisions. For instance, in a platoon of vehicles which is following a curved path using control law designed for objective (5), if a vehicle starts veering out and thus creating an emergency or abnormal condition, then changing the control law to satisfy objective (3) might prove to be a good way to solve the problem.

In the studies for longitudinal control and platooning, it is generally assumed that the road can provide necessary forces as determined by the controller. This assumption implies that either the vehicle is operating in a range such that the vehicle can respond using only a tractionless control, or that a reliable traction control is in place.

The dynamics for the system are highly nonlinear and time varying, which motivates the use of sliding mode control strategy [13] to follow a target slip. Lyapunov stability theorem based [15, 16] and sliding mode based [17, 18, 19] controllers have been assessed by researchers. The sliding mode controller designed for vehicle traction control is made adaptive to reduce the control discontinuity around the switching surface of the sliding mode. Sliding mode based scheme is also used to estimate the road tire conditions for maximum acceleration and maximum deceleration. The main problem with sliding mode control is the high frequency chattering across the switching surface[13]. A boundary layer is introduced around the switching surface and an appropriate function is used in the controller to reduce chattering.

Tractionless controllers can become unstable in the presence of external disturbances. Traction controllers, on the other hand, handle disturbances well. Simulations were performed on various road conditions to compare the performances of the two types of controllers. A simulation study was also performed to compare the effects of wind

disturbance on the two types of controllers for longitudinal control of vehicles. The results of the study are given in section-10 of this paper, which confirm the advantage of using traction control.

2. Background

To design a good controller, a representative mathematical model of the system is needed. In this section, a mathematical model for vehicle traction control is described [5, 6, 17, 18, 19] for analysis of the system, design of control laws, and computer simulations. Although, the model considered here is relatively simple, it retains the essential dynamic elements of the system.

Understanding of stability is essential for design of a good control system. The stability of the system, described in this section, is analyzed by linearizing the system around the equilibrium point.

2.1 System Dynamics

A vehicle model, which is appropriate for both acceleration and deceleration, is described in this sub-section. The model identifies wheel speed and vehicle speed as state variables and wheel torque as the input variable. The two state variables in this model are associated with one-wheel rotational dynamics and linear vehicle dynamics. The wheel dynamics and vehicle dynamics are derived by applying Newton's law.

2.1.1 Wheel Dynamics

The dynamic equation for the angular motion of the wheel is

$$\dot{\omega}_w = [T_e - T_b - R_w F_t - R_w F_w]/J_w \qquad (1)$$

where J_w is the moment of inertia of the wheel, ω_w is the angular velocity of the wheel, the over dot indicates differentiation with respect to time, and the other quantities are as defined in Table 1. The total torque acting on the wheel divided by the moment of inertia of the wheel equals the wheel angular acceleration. The total torque consists of shaft torque from the engine, which is opposed by the brake torque and the torque components due to the tire tractive force and the wheel viscous friction force. The wheel viscous friction force, a function of the wheel angular velocity, is the friction force developed on the tire-road contact surface. The tractive force developed on the tire-road contact surface is dependent on the wheel slip, the difference between the vehicle speed and the wheel speed, normal&d by the vehicle speed for braking and the wheel speed for acceleration (see Eq. (2)). The engine torque and the effective moment of inertia of the driving wheel depend on the transmission gear shifts.

R_w	Radius of the wheel
N_y	Normal reaction force from the ground
T_e	Shaft torque from the engine
T_b	Brake torque
F_x	Tractive force
F_w	Wheel viscous friction

Table 1 Wheel Parameters

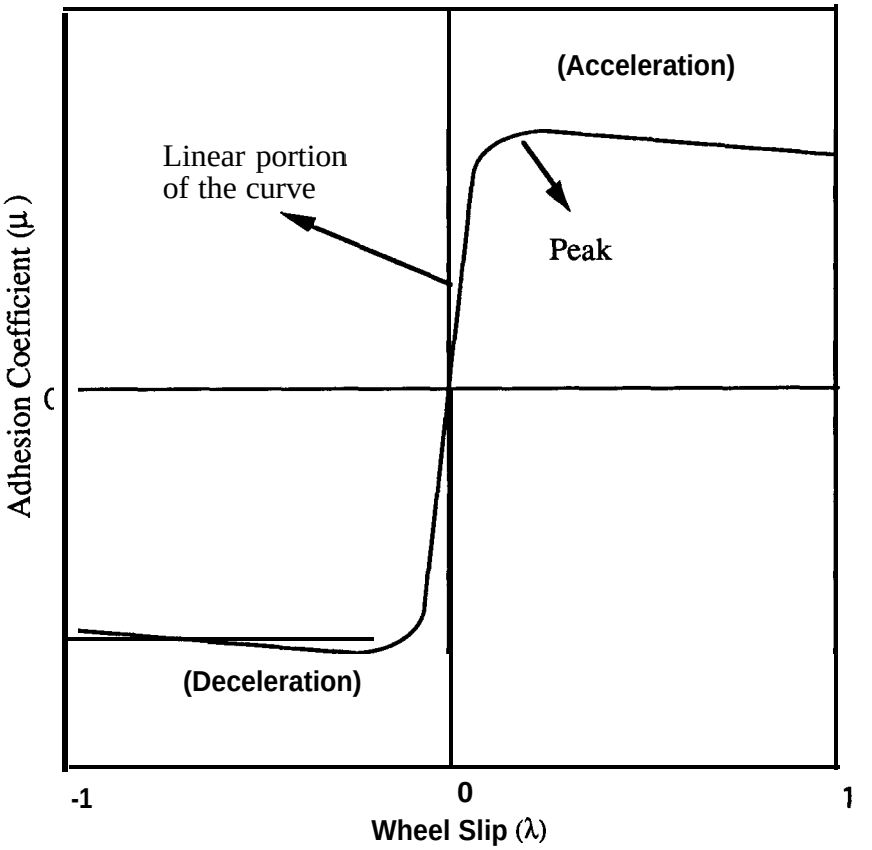

Figure 1 A typical $\mu-\lambda$ Curve

Applying a driving torque or a braking torque to a pneumatic tire produces tractive force at the tire-ground contact patch [14, 20]. The driving torque produces compression at the tire tread in front of and within the contact patch. Consequently, the tire travels less distance than it would if it were free rolling. In the same way, when a braking torque is applied, it produces tension at the tire tread within the contact patch and at the front. Because of this tension, the tire travels more distance than it would if it were free rolling. This phenomenon is referred to as the deformation slip or wheel slip [14, 17, 18, 19,201. The adhesion coefficient $\mu(\lambda)$ is a function of wheel slip λ. Figure 1 shows a typical $\mu-\lambda$ curve. References [17, 18 and 19] are the sources for the typical curve and [8] gives a more mathematical description of the tire model. Mathematically, wheel slip is defmed as

$$\lambda = (\omega_w - \omega_v)/\omega, \omega \neq 0 \qquad (2)$$

where, ω_v is vehicle angular velocity defined as

$$\omega_v = \frac{V}{R_w} \tag{3}$$

which is equal to the linear vehicle velocity, V, divided by the radius of the wheel. The variable ω is defined as

$$\omega = \max(\omega_w, \omega_v) = \begin{cases} \omega_w \text{ for } \omega_w \geq \omega_v \\ \omega_v \text{ for } \omega_w < \omega_v \end{cases} \tag{4}$$

which is the maximum of vehicle angular velocity and wheel angular velocity.

The tire tractive force is given by

$$F_t = \mu(\lambda) N_v \tag{5}$$

where the normal tire force, N,, depends on vehicle parameters such as the mass of the vehicle, location of the center of gravity of the vehicle, and the steering and suspension dynamics. The adhesion coefficient, which is the ratio between the tractive force and the normal load, depends on the road-tire conditions and the value of the wheel slip **[5,17].** For various road conditions, the curves have different peak values and slopes, as shown in Figure 2. The adhesion coefficient-slip characteristics are influenced by operational parameters like speed and vertical load. The average peak values for various road surface conditions are shown in Table 2 1141.

Surface	Average Peak Value
Asphalt and concrete (dry)	0.8-0.9
Asphalt (wet)	0.5-0.6
Concrete (wet)	0.8
Earth road (dry)	0.68
Earth road (wet)	0.55
Gravel	0.6
Ice	0.1
Snow (hard packed)	0.2

Table 2 Average Peak Values for Adhesion Coefficient

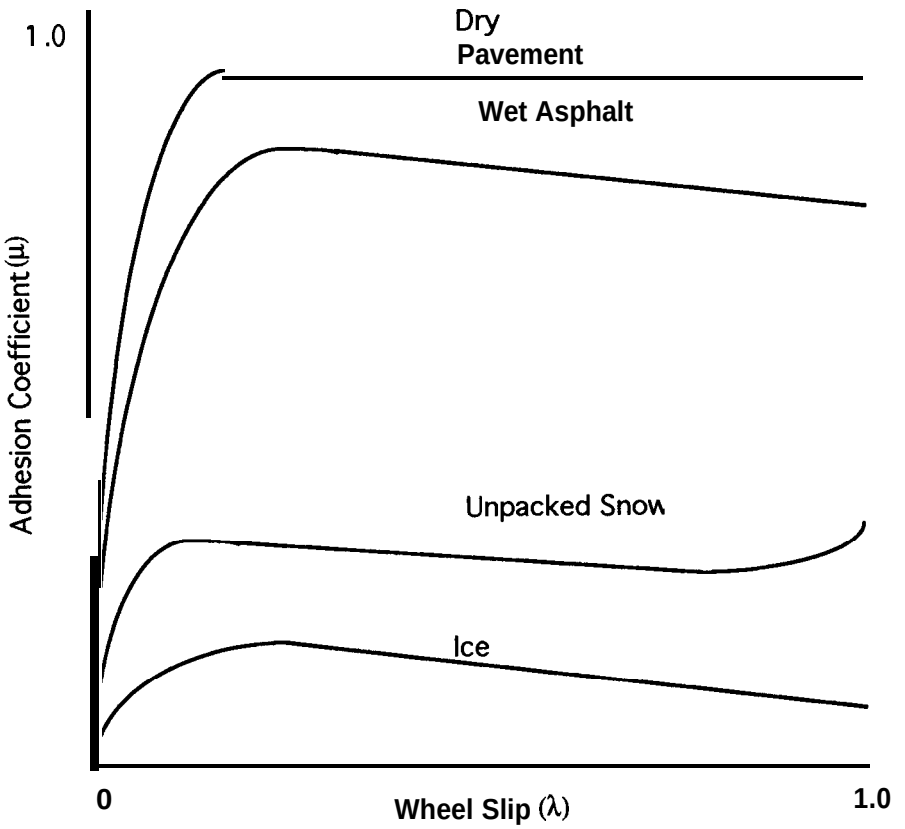

Figure 2 $\mu-\lambda$ Curves for Different Road Conditions

The model for wheel dynamics is shown in Figure 3. The parameters in this figure are defined in Table 1. The figure shows the acceleration case for which the tractive force and wheel viscous friction force are directed toward the motion. The wheel is rotating in the clockwise motion and slipping against the ground, i.e. $\omega_w > \omega_v$. The slipping produces the tractive force towards right causing the vehicle to accelerate towards right. In the case of deceleration, the wheel still rotates in the clockwise motion but skids against the ground, i.e. $\omega_w < \omega_v$. The skidding produces the tractive force towards left causing the vehicle to decelerate.

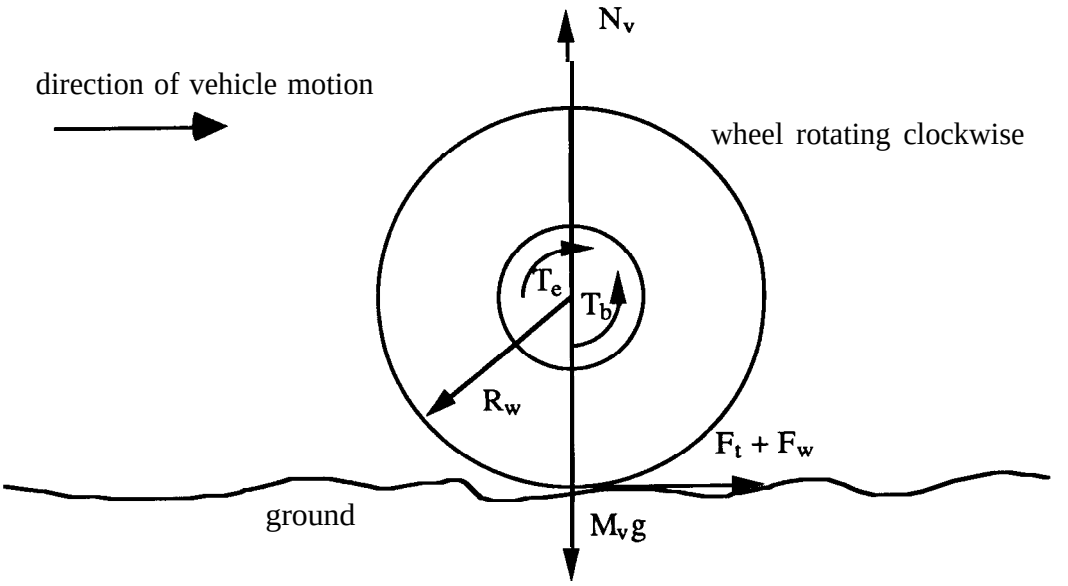

Figure 3 Wheel Dynamics

2.1.2 Vehicle Dynamics

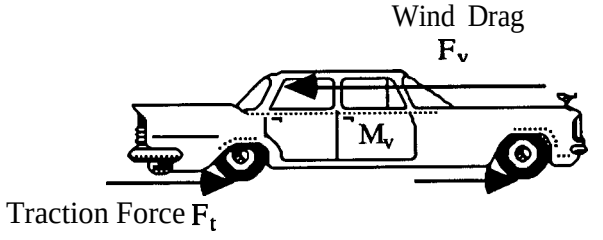

Figure 4 Vehicle Dynamics

The vehicle model considered for the system dynamics is shown in Figure 4. The parameters in the figure are defined as:

F_v : Wind drag force (function of vehicle velocity)

M_v : Vehicle mass

N_w : Number of driving wheels (during acceleration) or the total number of wheels (during braking).

The linear acceleration of the vehicle is governed by the tractive forces from the wheels and the aerodynamic friction force. The n-active force, F_t, is the average friction

force of the driving wheels for acceleration and the average friction force of all wheels for deceleration. The dynamic equation for the vehicle motion is

$$\dot{V} = [N_w F_t - F_v]/M_v \tag{6}$$

The linear acceleration of the vehicle is equal to the difference between the total tractive force available at the tire-road contact and the aerodynamic drag on the vehicle, divided by the mass of the vehicle. The total tractive force is equal to the product of the average friction force, F_t and the number of relevant wheels, N_w. The aerodynamic drag is a nonlinear function of the vehicle velocity and is highly dependent on weather conditions. It is usually proportional to the square of the vehicle velocity.

2.1.3 Combined System

The dynamic equation of the whole system can be written in state variable form by defining convenient state variables. By defining the state variables as

$$x_1 = \frac{V}{R_w} \tag{7}$$

$$x_2 = \omega_w \tag{8}$$

and denoting x = max (x_1,x_2), we can rewrite Equations (1) and (6) as

$$\dot{x}_1 = -f_1(x_1) + b_{1N}\,\mu(\lambda) \tag{9}$$

$$\dot{x}_2 = -f_2(x_2) - b_{2N}\,\mu(\lambda) + b_3 T \tag{10}$$

where

$$T = T_e - T_b$$

$$\lambda = (x_2 - x_1)/x)$$

$$f_1(x_1) = [F_v(R_w x_1)]/(M_v R_w)$$

$$b_{1N} = N_v N_w/(M_v R_w)$$

$$f_2(x_2) = R_W F_W(x_2)/J_W$$

$$b_{2N} = R_w N_v/J_w$$

$$b_3 = 1/J_w \tag{11}$$

The combined dynamic system can be represented as shown in the Figure 5. The control input is the applied torque at the wheels, which is equal to the difference between the shaft torque from the engine and the braking torque. During acceleration, engine torque is the primary input where as during deceleration, the braking torque is the primary input.

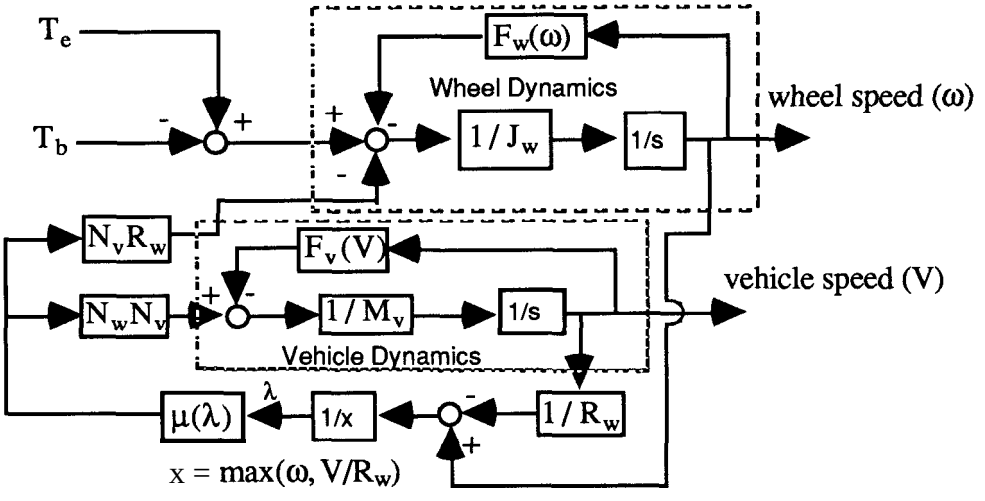

Figure 5 Vehicle/Brake/Road Dynamics: One-Wheel Model

2.1.4 System Dynamics In Terms Of Slip

Wheel slip is chosen as the controlled variable for traction control algorithms because of its strong influence on the tractive force between the tire and the road. Wheel slip is calculated from Equation (3) by using the measurements of wheel angular velocity and the estimated value of the vehicle velocity from either the accelerometer data or the magnetic marker data, as explained in the Introduction. By controlling the wheel slip, we control the tractive force to obtain desired output from the system. In order to control the wheel slip, it is convenient to have system dynamic equations in terms of wheel slip. Since the functional relationship between the wheel slip and the state variables is different for acceleration and deceleration, the equations for the two cases are described separately in the following sub-sections.

Acceleration Case

During acceleration, condition $x_2 > x_1, (x_2 \neq 0)$ is satisfied and therefore

$$\lambda = (x_2 - x_1)/x_2 \tag{12}$$

Differentiating this equation, we obtain

$$\lambda = [(1 - \lambda)\dot{x}_2 - \dot{x}_1]/x_2 \tag{13}$$

Substituting Equations (9), (10) and (12) into Equation (13), we obtain

$$\lambda = [\,[f_1(x_1) - (1 - \lambda)f_2(x_2)] - [(1 - \lambda)b_{2N} + b_{1N}]\mu + (1 - \lambda)b_3T]/x_2 \tag{14}$$

which is the wheel slip dynamic equation during acceleration. This equation is highly nonlinear and involves uncertainties in its parameters. The non linearity of the equation is caused by the following factors: (1) the relationship between wheel slip and wheel velocity and vehicle velocity is nonlinear, (2) the $\mu-\lambda$ relationship is nonlinear, (3) there are multiplicative terms like $(1 - \lambda)b_{2N}\mu/x_2$ and $(1 - \lambda)b_3T/x_2$ in the equation, and (4) functions $f_1(x_1)$ and $f_2(x_2$ are nonlinear.

Deceleration Case

During deceleration, condition $x_2 \leq x_1, (x_1 \neq 0)$ is satisfied, and therefore wheel slip is defined as:

$$\lambda = (x_2 - x_1)/x_1 \tag{15}$$

Differentiating this equation, we obtain

$$\lambda = [\dot{x}_2 - (1 + \lambda)\dot{x}_1]/x_1 \tag{16}$$

Substituting Equations (9), (10) and (15) into Equation (16), we obtain

$$\lambda = [\,[(1 + \lambda)f_1(x_1) - f_2(x_2)] - [b_{2N} + (1 + \lambda)b_{1N}]\mu + b_3T]/x_1 \tag{17}$$

This gives the wheel slip dynamic equation for deceleration case. This equation is also highly nonlinear and involves uncertainties like Equation (14).

2.2 SYSTEM STABILITY

The local stability of a nonlinear system can be studied by linearizing the system around its equilibrium point. Therefore, in this section, the vehicle nonlinear system equations are linearized around the equilibrium point in order to study the system stability. The equilibrium point (x_{10},x_{20}) of the vehicle system described by Equations (9) and (10) can be obtained by equating the right hand sides of the two equations to zero.

Acceleration Case

For the acceleration case, the Jacobian matrix at equilibrium is:

$$A = \begin{bmatrix} -\frac{df_1}{dx_1}(x_{10}) - b_{1N}\frac{\partial \mu}{\partial \lambda}(x_{10},x_{20})/x_{20}, & b_{1N}\frac{\partial \mu}{\partial \lambda}(x_{10},x_{20})\frac{x_{10}}{x_{20}^2} \\ b_{2N}\frac{\partial \mu}{\partial \lambda}(x_{10},x_{20})/x_{20}, & -\frac{df_2}{dx_2}(x_{20}) - b_{2N}\frac{\partial \mu}{\partial \lambda}(x_{10},x_{20})\frac{x_{10}}{x_{20}^2} \end{bmatrix} \qquad (18)$$

The eigenvalues of A are obtained by solving for λ_e in the equation

$$\det(\lambda_e I - A) = 0 \qquad (19)$$

The sign of the real part of the eigenvalues determines the stability of the linearized system. The real part of the eigenvalues is calculated to be

$$-\frac{\left[\frac{df_1}{dx_1}(x_{10}) + \frac{df_2}{dx_2}(x_{20}) + \frac{\partial \mu}{\partial \lambda}(x_{10},x_{20})\left[b_{1N}/x_{20} + b_{2N}\frac{x_{10}}{x_{20}^2}\right]\right]}{2}$$

Notice that $df_1/dx_1, df_2/dx_2, x_1, x_2, b_{1N}$ and b_{2N} are all positive. When $\partial\mu/\partial\lambda$ is positive, the eigenvalues of A have negative real parts, and when $\partial\mu/\partial\lambda$ is negative, the eigenvalues of A have positive real parts for

$$\left[b_{1N}/x_{20} + b_{2N}\frac{x_{10}}{x_{20}^2}\right] > \frac{\frac{df_1}{dx_1}(x_{10}) + \frac{df_2}{dx_2}(x_{20})}{\left|\frac{\partial \mu}{\partial \lambda}\right|} \qquad (20)$$

Hence, under the condition (20) the system is unstable.

Deceleration Case

For the deceleration case, the Jacobian matrix at the equilibrium is:

$$A = \begin{bmatrix} -\frac{df_1}{dx_1}(x_{10}) - b_{1N}\frac{\partial\mu}{\partial\lambda}(x_{10},x_{20})\frac{x_{20}}{x_{10}^2}, & b_{1N}\frac{\partial\mu}{\partial\lambda}(x_{10},x_{20})\frac{1}{x_{10}} \\ b_{2N}\frac{\partial\mu}{\partial\lambda}(x_{10},x_{20})\frac{x_{20}}{x_{10}^2}, & -\frac{df_2}{dx_2}(x_{20}) - b_{2N}\frac{\partial\mu}{\partial\lambda}(x_{10},x_{20})\frac{1}{x_{10}} \end{bmatrix} \quad (21)$$

The real part of the eigenvalues of A is calculated to be

$$\frac{-\left[\frac{df_1}{dx_1}(x_{10}) + \frac{df_2}{dx_2}(x_{20}) + \frac{\partial\mu}{\partial\lambda}(x_{10},x_{20})\left[b_{1N}\frac{x_{20}}{x_{10}^2} + b_{2N}\frac{1}{x_{10}}\right]\right]}{2}$$

Here also $df_1/dx_1, df_2/dx_2, x_1, x_2, b_{1N}$ and b_{2N} are all positive, so when $\partial\mu/\partial\lambda$ is positive, the eigenvalues of A have negative real parts. When $\partial\mu/\partial\lambda$ is negative, the eigenvalues of A have positive real parts for

$$\left[b_{1N}\frac{x_{20}}{x_{10}^2} + b_{2N}/x_{10}\right] > \frac{\frac{df_1}{dx_1}(x_{10}) + \frac{df_2}{dx_2}(x_{20})}{\left|\frac{\partial\mu}{\partial\lambda}\right|} \quad (22)$$

Therefore, under condition (22) the system is unstable.

3. Slip Control

Longitudinal traction can be controlled by controlling wheel slip. A nonlinear control strategy based on sliding mode, which is robust to parametric uncertainties, is chosen for slip control.

3.1 Sliding Mode Control of the Wheel Slip

The following is the derivation of the sliding mode control law for wheel slip

regulation.

The slip dynamic equation for acceleration (13) can be written as

$$\dot{\lambda} = f + bu \tag{23}$$

where

$$f = \frac{1}{x_2}[f_1(x_1) - (1 - \lambda)(f_2(x_2) + b_{2N}\mu(\lambda)) - b_{1N}\mu(\lambda)] \tag{24}$$

$$u = \frac{(1 - \lambda)}{x_2}T, \tag{25}$$

and

$$b = b_3 \tag{26}$$

Define the switching surface S(t) by equating the sliding variable, s defined below to zero.

$$s = \lambda_e \tag{27}$$

where $\lambda_e = \lambda - \lambda_d$ and λ_d is the desired slip. The nonlinear function f is estimated as $\hat{f}$, and the estimation error on f is assumed to be bounded by some known function $F=F(x)$, so that $|f - \hat{f}| \le F$. The control gain b is bounded as $0 \le b_{min} \le b \le b_{max}$. The control gain b and its bounds can be time varying or state dependent. Since the control input is multiplied by the control gain in the dynamics, the geometric mean of the lower and upper bounds of the gain, $\hat{b} = \sqrt{b_{max} b_{min}}$, is taken as the estimate of b. The bounds can also be written as $\alpha^{-1} \le \hat{b}/b \le \alpha$, where $\alpha = \sqrt{b_{max}/b_{min}}$. The controller is designed as

$$T = \frac{x_2}{(1 - \lambda)}u \tag{28}$$

where

$$u = \hat{b}^{-1}[\hat{u} - k\,\mathrm{sgn}(s)] \tag{29}$$

and

$$\hat{u} = -\hat{f} + \dot{\lambda}_d - c\lambda_e \qquad c = \text{constant} > 0 \tag{30}$$

A finite time $(\le \lambda_e(0)/\eta)$ is taken to reach the switching surface and the stability of the system is guaranteed with an exponential convergence once the switching surface is encountered, if we choose the sliding gain as

$$k \ge \alpha(F + \eta) + (\alpha - 1)|\hat{u}| \tag{31}$$

Switching control laws are known to be not practical to implement because of

chattering [13]. Chattering is caused by non-ideal switching of the s variable around the switching surface. Delay in digital implementation causes s to pass to the other side of the surface S(t), which in turn produces chattering. A practical method for avoiding chattering is to introduce a region around S(t) so that s changes its value continuously [13]. In the present work, we define a boundary of a fixed width ϕ around the switching surface and define the function int(.) as:

$$\text{int}(a,j,s,\phi) = as/\phi + \frac{j}{\phi}\int_0^t sdt \quad \text{for } |s| \le \phi$$

$$\text{int}(a,j,s,\phi) = \text{sgn}(s) \text{ otherwise} \tag{32}$$

The parameters a and j are

$$a = 2\gamma\phi/k(x_d)$$

$$j = \gamma^2\phi/k(x_d) \tag{33}$$

and u is changed to

$$u = \hat{b}^{-1}[\hat{u} - k\ \text{int}(a,j,s,\phi)] \tag{34}$$

The bandwidth of the filter for variable s is given by γ.

Notice that the second term in (34) acts as a PI controller in the region $|s| < \phi$. The first term is given by (30) which attempts to cancel the nonlinear term in (23) and further adds the desired dynamics. If the cancellation of the nonlinear term is perfect, i.e. $f - (\hat{b}/\hat{b})\hat{f} = 0$, Equations (23), (30), (32) and (34) will result in a linear error equation with no forcing term, which implies that the slip error and the integral of the slip error as well as the sliding variable, s, all converge to zero. However, the cancellation can never be perfect, which can be easily understood by the presence of $\mu(\lambda)$ in Equation (24). The integrator can absorb the error due to imperfect cancellation and assures a superior performance.

In the later portion of this report, sliding mode control will be utilized for longitudinal platoon control, and the associated control variable will include a term proportional to the integral of the error, introduced by the int(.) function. It should be noted that the consideration given above will apply to longitudinal platoon control also.

For deceleration, we can obtain the system in the form of Eq. (23) by defining f, u andbas

$$f = [(1 + \lambda)f_1(x_1) - f_2(x_2)] - [b_{2N} + (1 + \lambda)\, b_{1N}]\mu]/x_1 \quad (35)$$

$$u = T/x_1 \quad (36)$$

and

$$b = b_3 \quad (37)$$

Following the same steps as for the acceleration case, the control law for deceleration is also given by Equations (28-3 1).

3.2 Adaptive Sliding Mode Control Design

To reduce the amount of control discontinuity due to uncertainties in b, the above described scheme can be made adaptive. It is assumed that b is a constant or a slowly varying parameter. Adaptation is applied only outside the boundary layer so that the effect of noise on adaptation is minimal [12]. For the system described by Eqs. (23-25), we define

$$As = s - \beta(.)int(a,j,s,\phi), \quad (38)$$

where

$$\beta(.) = \phi/[a + \frac{j}{s}\int_0^t sdt] \quad (39)$$

Notice that within the boundary, As = 0, and outside the boundary,

$$As = s - [\phi/a]sgn(s) \quad (40)$$

because the integral is reset to zero every time s goes outside the boundary. The variable a is equated to one outside the boundary. Define a Lyapunov function candidate

$$V = \frac{(\Delta s)^2}{2} + \frac{(b - \hat{b})^2}{2} \quad (41)$$

Differentiating and rearranging terms, we obtain

$$\dot{V} \leq -\eta|\Delta s| \quad (42)$$

when

$$k \geq \alpha(F + \eta) \tag{43}$$

and

$$\dot{\hat{b}} = -\frac{\hat{u}}{\hat{b}}\Delta s \tag{44}$$

The adaptation law is given by Equation (44). The block diagram of the controller is shown in Figure 6. In this figure, D refers to the Laplace operator and the dashed line shows the adjustment of $\hat{b}$.

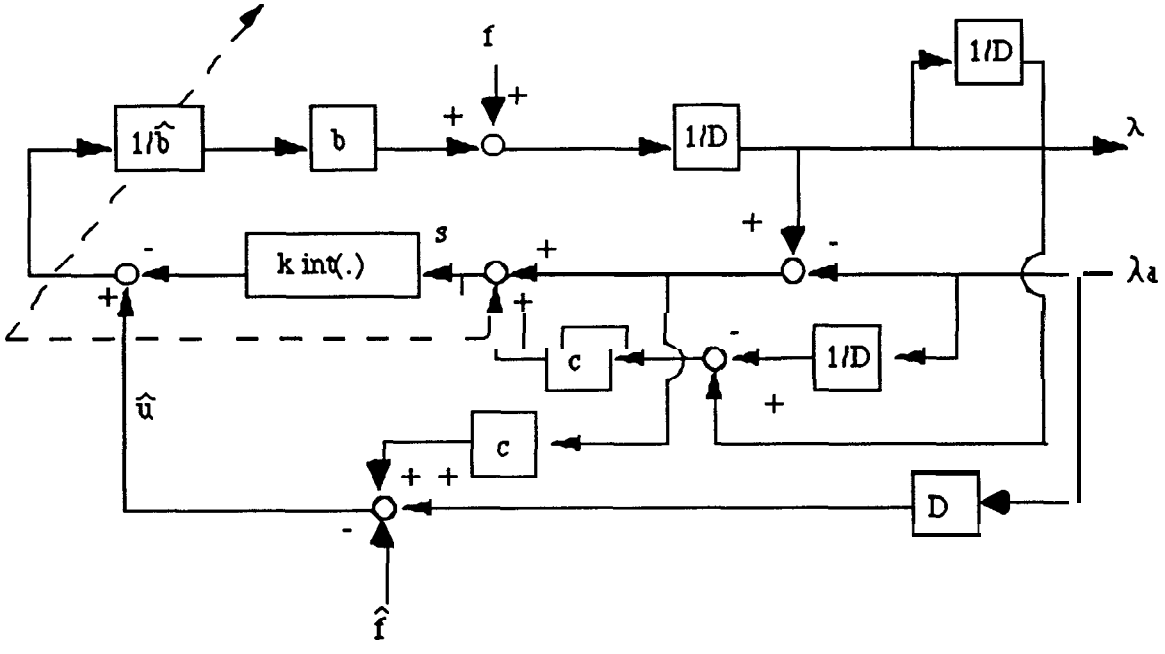

Figure 6 Block Diagram of the Traction Control

4. Optimal Time Control

The tire/road surface contact can be characterized by the local slope of the $\mu - \lambda$ curve. Maximum u-active force occurs at the peak of the curve where $\partial\mu/\partial\lambda$ is zero. Maximum positive tractive force is achieved at the positive peak of the curve and is desirable in order to achieve maximum acceleration. Maximum tractive force in the reverse direction is achieved at the negative peak of the curve and is desired for maximum deceleration. The

acceptable operating zone for the wheel slip is between the peak slips where the slopes are positive; outside this zone, the slopes are negative. To produce the fastest acceleration or deceleration, which can be seen as minimum-time control, the wheel slip should be regulated where the adhesion coefficient attains the peak value: a positive peak value for acceleration and a negative peak value for deceleration. The derivation of this optimal formulation is given in the appendix section of Tan's thesis [17]. A method to estimate the slope of the $\mu - \lambda$ curve, based on a single parameter sliding mode parameter estimation scheme is described below. The algorithm is based on estimating the slope of the $\mu - \lambda$ curve and then moving the target slip in the direction of the peak slip, until the peak slip is reached.

The minimum time acceleration and minimum time deceleration control can be employed in a single vehicle system In an automated highway system where a platoon of vehicles is to be controlled, minimum time acceleration and minimum time deceleration are not generally the best performance index.

4.1 Estimation

This section explains how to use the sliding mode parameter estimation to identify the local slope of the $\mu - \lambda$ curve, $\partial\mu/\partial\lambda$, from the estimations of μ and λ. In practice, the adhesion coefficient, μ, can be regarded as a function of time (road changes) and of slip (operating condition variations), i.e. $\mu = \mu(\lambda, t)$. Under the assumption that the road condition changes either slowly or suddenly, $\partial\mu/\partial\lambda$ can be approximated by

$$\frac{\partial\mu}{\partial\lambda}(t_k) \cong \frac{d\mu}{d\lambda}(t_k) \cong \frac{\Delta\mu(t_k)}{\Delta\lambda(t_k)} \qquad (45)$$

for virtually all time instants t_k, where $\Delta\mu$ and Ah are the differences between two adjacent sampling instants of μ and λ, respectively.

To obtain the value of $\Delta\mu$, we differentiate Equation (9) and rearrange terms.

$$\frac{\partial \mu}{\partial \lambda} = [\ddot{x}_1 + \frac{\partial f_1}{\partial x_1}\dot{x}_1]\frac{1}{b_{1N}\dot{\lambda}} \cong \frac{\Delta \mu}{\Delta \lambda} \tag{46}$$

Since the second term inside the bracket is usually insignificant compared with the first term, and the first term can be approximated by the difference of vehicle velocities at two consecutive sampling time instants divided by the sample time interval, we can approximate $\Delta\hat{\mu}$ as

$$\Delta\hat{\mu} = [\dot{x}_1(t_k) - \dot{x}_1(t_{k-1})]\frac{1}{b_{1N}} \tag{47}$$

An alternate estimation scheme could be based on differentiating Equation (10) instead of Equation (9).

The slope is estimated by using the sliding mode parameter estimation scheme. The parameter is updated according to

$$\frac{\dot{\partial \hat{\mu}}}{\partial \lambda}(t) = -k'\Delta\hat{\lambda}(t)\text{msat}(a',e,\phi') \tag{48}$$

where k' is the estimator gain and ϕ' is the boundary width across the switching surface. The switching surface is described by

$$e = O \tag{49}$$

where e is the prediction error defined as

$$e = \Delta\hat{\mu} - \frac{\dot{\partial \hat{\mu}}}{\partial \lambda}\Delta\hat{\lambda} \tag{50}$$

The msat(.) function is defined as

$$\text{msat}(a',e,\phi') = a'e/\phi' \qquad \text{for } |e| < \phi$$

$$\text{msat}(a',e,\phi') = \text{sgn}(e) \qquad \text{otherwise} \tag{51}$$

This function, instead of the signum function, is used here to reduce chattering. The variable a' is designed to provide a constant bandwidth filter which removes the high frequency chattering components, by choosing

$$a' = \gamma\phi/[(\Delta\hat{\lambda})^2 k'] \quad \text{if } \Delta\hat{\lambda} \geq \sqrt{\gamma\phi/(a'_{max})k'}$$

$$a' = a'_{max} \quad \text{if } \Delta\hat{\lambda} < \sqrt{\gamma\phi/(a'_{max})k'} \tag{52}$$

where γ is the desired constant bandwidth of the filter, and a'_{max} is the maximum value of

the variable a'.

4.2 Target Update Algorithm

We can utilize the sign of the current $\partial\mu/\partial\lambda$, which is the output of the sliding mode parameter estimation process, to reach the peak slip. This information reveals the direction of the peak slip from the present position of λ. For example, if the slope is positive at $\lambda(t_k)$, we know that the present slip is within the positive slope region. We therefore propose a simple and practical method for updating the estimated peak slips based on the sign of the estimated slope. The proposed method contains the following basic steps: (1) Move the target slip in the estimated direction towards the peak slip. (2) Steer the wheel slip toward the new target slip via the sliding mode slip tracking algorithm. (3) At the same time, estimate the new local slope in the $\mu - \lambda$ curve and then return to step 1. The algorithm designed to move the target slip toward the peak slip (step 1) is called the target update algorithm.

The target slip is updated according to the following algorithm. The target slip is moved in the direction of the peak according to the sign of the slope of the $\mu - \lambda$ curve. The step size remains the same if the sign of the slope does not change, and the step size is halved if the sign changes. The target is updated according to

$$\lambda_T(k+1) = \lambda_T(k) - (-1)^n \mathrm{sgn}\left(\widehat{\frac{\partial\mu}{\partial\lambda}}\right)\mathrm{step}(k), \text{ when } (-1)^n\lambda(k) < 0 \tag{53}$$

where, if the sign of the estimated slope at the (k+l)st instant is different from the one estimated at the kth instant, then

$$\mathrm{step}(k+l) = \mathrm{step}(k)/2 \tag{54}$$

and if the sign is same then

$$\mathrm{step}(k+l) = \mathrm{step}(k) \tag{55}$$

The step size is initialized at a convenient value.

$$\mathrm{step}(O) = a \tag{56}$$

For varying road conditions, either the step size should have a lower bound or it should be re-initialized if the value of the estimated slope varies substantially after a steady value has been reached. This is important because otherwise the estimation process would cease. Notice in Equation (53) that n = 1 is the acceleration case and n = 2 is the deceleration case.

4.3 Chattering Due To Target Updating

Chattering is observed when using the combined algorithm. This chattering should not be confused with the sliding mode chattering for which a solution has been proposed. This chattering is due to rapid updating of the target slip. In order to smooth the control, the algorithm is modified such that the target is updated only when $|s| c \varepsilon$, where s is the sliding variable used in slip control and ε is chosen to be some small positive number which gives the desired smoothness.

5. Anti-Spin Acceleration and Anti-Skid Braking

For anti-spin acceleration and anti-skid braking, the wheel slip should be maintained at the positive slope region of the $\mu - \lambda$ curve. To accomplish this, we can use the estimation scheme described in the last section. To obtain anti-spin acceleration, if the current wheel slip is in the negative slope region, the target slip should be decremented, and if the wheel slip is in the positive slope region, the target slip is not changed. Similarly, to obtain anti-skid deceleration, if the current wheel slip is in the negative slope region, the target slip should be incremented, and if the wheel slip is in the positive slope region, the target slip is not changed.

When the aim of a traction control system is only anti-skid braking and anti-spin acceleration without any demands on velocity or time, the ultimate control objective is not the regulation of the wheel slip itself. The wheel slip should not enter the negative slope

region. From this point of view, a fuzzy rule-based control approach would also be attractive and well suited.

6. Maximum Steerability in Lateral Control

Although maximum traction is desirable for optimum time control while decelerating in straight line braking, a trade off between stability and stopping distance may be necessary during combined hard braking and severe steering maneuvers. In these type of maneuvers, understeered vehicles - even those equipped with ABS - will oversteer and spin out. A previous study [15,16] shows that for lateral control of a vehicle while decelerating, the best cornering performance and steerability of the vehicle can be attained by maintaining the longitudinal wheel slip at the values given by Equations (57) and (58). The cornering performance and steerability of the vehicle is measured by the smallest turning radius without loss of stability, combined with the shortest stopping distance.

$$\lambda_{fT} = ae^{b|\delta s|} \tag{57}$$

$$\lambda_{rT} = ce^{d|\delta s|} \tag{58}$$

In the equations, δs is the forward steering angle; a, b, c and d are constants, the optimum values of which can be obtained by simulations, and finally, λ_{fT} and λ_{rT} are the front and the rear target slip values. These equations were obtained from analysis of simulation results, conducted by Taheri [16], where different combinations of desired front and rear slip values were used. It was found that the best combination of desired slip values, in terms of cornering performance and steerability, could be represented by exponential functions of the front wheel steering angle. To control the wheel slips at these values, the traction controller designed in section 3 can be used.

7. Longitudinal Platoon Control

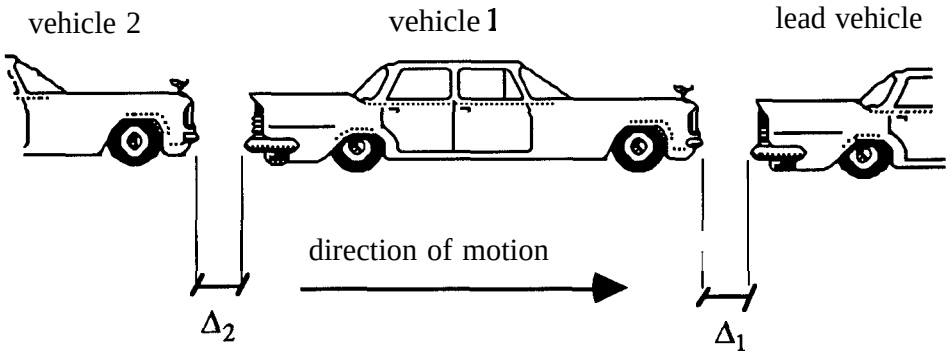

Δ_i, i = 1,2... are the spacing between consecutive vehicles

Figure 7 Platoon of vehicles

Longitudinal control strategies are necessary in order to regulate the spacing and velocity of vehicles in an automated highway system consisting of a platoon of vehicles (see Figure 7). The longitudinal control algorithm must maintain the spacing policy under normal maneuvers such as acceleration, deceleration, turning, and merging. The controller must also insure good performance over a variety of operating points and external conditions without sacrificing safety or reliability.

The control to maintain a vehicle behind another vehicle at specified spacing in a longitudinal platoon is obtained by using two sliding surfaces, one for tracking the vehicle velocity, and the other to obtain the input torque. This " two surface" method [4] is used for systems with relative degree greater than one. The technique is discussed below.

Let s_1 be the first sliding surface defined as

$$s_1 = \dot{\varepsilon} + c_1\varepsilon \tag{59}$$

where ε is the spacing error between the vehicle being controlled and the vehicle in front. The spacing error is defined as the difference between the actual distance between the two vehicles and the desired distance between them. When the desired distance between the two vehicles is a constant, $\dot{\varepsilon}$ becomes the velocity error between the vehicle to be controlled and the vehicle in front. Differentiation of Equation (59) yields

$$\dot{s}_1 = \ddot{\varepsilon} + c_1\dot{\varepsilon} \tag{60}$$

where $\ddot{\varepsilon} = \dot{x}_1 - \dot{x}_{1des}$, and x_{1des} is the desired xl, which is equal to the velocity of the front vehicle for a constant desired spacing. For the first sliding surface, $\mu(\lambda)$ is the control input, which is further controlled by the second sliding surface using the system control input T. Using the sliding mode design procedure and introducing $-ksgn(s_1)$ term for robustness, we obtain

$$\dot{s}_1 = \dot{x}_1 - \dot{x}_{1des} + c_1\varepsilon = -ksgn(s_1) \tag{61}$$

Substituting $\dot{x}_1$ by the estimated quantities in the right hand side of Equation (9) yields

$$-\hat{f}_1(x_1) + \hat{b}_{1N}\hat{\mu}(\lambda) = \dot{x}_{1des} - c_1\dot{\varepsilon} - ksgn(s_1) \tag{62}$$

From this equation, we obtain the desired adhesion value, $\hat{\mu}(\lambda)$.

$$\hat{\mu}(\lambda) = \frac{1}{\hat{b}_{1N}}\left[\dot{x}_{1des} + \hat{f}_1(x_1) - c_1\dot{\varepsilon} - ksgn(s_1)\right] \tag{63}$$

From the desired adhesion value, the desired slip value λ_{des} can be calculated using the $\mu - \lambda$ curve. Since the actual curve is not known, we use a nominal $\mu - \lambda$ curve. The error in the estimated and actual μ value is denoted by $\mu_e(\lambda)$. The sliding gain of the first surface can overcome this error by utilizing the bounds on $b_{1N}\mu_e(\lambda)$. The estimated value of $f_1(x_1)$ in the Equations (62) and (63) is shown by $\hat{f}_1(x_1)$. For chattering reduction, the function sgn(.) is replaced by int(.). Here also, the control law can be made adaptive to reduce the discontinuity across the switching surface. To obtain the desired slip, we try to control the wheel slip directly at the desired value using the algorithm for slip-control, by defining the second sliding surface as

$$s_2 = \lambda_e \tag{64}$$

The design of the control law, using the second sliding surface, is the same as described in section 3.

In the platoon control problem, a decentralized control law is used for the special interconnection (platoon) of the nonlinear dynamical subsystems, each one representing a vehicle. The position errors can be obtained by integrating the velocity errors. Thus, for

each subsystem containing a vehicle in front and a following vehicle, sliding mode control guarantees the convergence of the spacing errors with a sum of finite and exponentially convergent time periods, so that the overall system is convergent with a rate of the slowest dynamical subsystem.

8 Longitudinal Traction with Lateral Control

The longitudinal traction control developed in this paper can be combined with some appropriate lateral control [8, 9] to satisfy the objective of building a complete motion control system. In a combined platoon vehicle system for PATH, the longitudinal spacing error between vehicles is controlled by the longitudinal controller, while the lateral deviation and the yaw rate are controlled by the lateral controller.

It is important to use traction control when longitudinal and lateral controllers are being implemented simultaneously, because wheel slip not only controls traction in the longitudinal direction, but also in the lateral direction. At high wheel slip values, there is less adhesion in the lateral direction and therefore, for lateral stability of the vehicle, the wheel slip values should be kept low.

9 Passive Control

Some studies for longitudinal control and platooning assume that either the road can provide necessary forces for the controller in the operating range or that a traction control is in place. This assumption implies that if the road can react sufficiently, passive or tractionless controllers can be used to satisfy the control objectives. Passive controllers do not explicitly take adhesion availability of the road-tire interaction into account and therefore their range of operation is limited as compared to the traction controllers. A simple PID control and a sliding mode based passive control are derived next.

A simple PID control of the form

$$T = -k_1\dot{\varepsilon} - k_2\varepsilon - k_3\int_0^t \varepsilon\, dt \tag{65}$$

tries to minimize the longitudinal spacing error ε between two vehicles without taking traction into account. Different weights are given to the proportional, derivative and integral terms based on experimental data. The tuning of the PID gains relies heavily on trial and error and the design is experimental rather than analytical. Hence, there is no stability proof for this control on the highly nonlinear model of the system.

A tractionless sliding mode controller, which tries to maintain the longitudinal spacing between vehicles, can be designed by differentiating Equation (9), so that the input variable appears in the equation. For instance, in the case of acceleration, we obtain

$$\ddot{x}_1 = \frac{-\partial f_1}{\partial x_1}\dot{x}_1 + b_{1N}\frac{\partial \mu}{\partial \lambda}[(1 - \lambda)\dot{x}_2 - \dot{x}_1]/x_2 \tag{66}$$

which can be written as

$$\ddot{x}_1 = F_1 + F_2 T \tag{67}$$

where

$$F_1 = \left[\frac{-\partial f_1}{\partial x_1} + b_{1N}\frac{\partial \mu}{\partial \lambda}\frac{1}{x_2}\right]\dot{x}_1 + b_{1N}\frac{\partial \mu}{\partial \lambda}(1 - \lambda)\frac{[-f_2(x_2) - b_{2N}\mu(\lambda)]}{x_2} \tag{68}$$

and

$$F_2 = b_{1N}\frac{\partial \mu}{\partial \lambda}\frac{(1 - \lambda)}{x_2}b_3 \tag{69}$$

If we let

$$s = \dot{\varepsilon} + c_1\varepsilon \tag{70}$$

where $\varepsilon = x_1 - x_{1des}$, the control law takes the form

$$T = \frac{1}{\hat{F}_2}\left[-\hat{F}_1 + \ddot{x}_{1des} - c_1\dot{\varepsilon} - k\ \mathrm{sgn}(s)\right] \tag{71}$$

where $\hat{F}_1$ is the estimate of F_1, and $\hat{F}_2$ is the estimate of F_2. Here also sgn(.) can be replaced by an appropriate function for chattering reduction and the sliding gain can be chosen appropriately to ensure convergence.

10. Numerical Simulations

A simulation study was performed for the acceleration case without any measurement noise. A typical μ-λ curve was assumed fixed for the whole test road surface. During acceleration, only the two wheels attached to the engine were considered, because the inertia of the other two is negligible. The vehicle parameters for simulation during acceleration are shown in Table 3.

Parameters	Values
mass of the vehicle (M_v)	1000 Kg
radius of the wheel (R,)	0.31 m
wheel inertia (I_w)	0.65 Kg m^2
engine inertia (I,)	0.429 Kg m^2
overall gear-ratio (r)	9.5285
normal tire force (N,)	2287 N
number of wheels (N,)	2
Equivalent wheel inertia	$I_w + I_e r^2/2$ Kg m^2
$f_1(x_1)$	cx_1^2 rad/sec^2, $c = 0.595(R_w/M_v)$
$f_2(x_2)$	0 rad/sec^2

Table 3 Simulation Parameters

In the simulations, velocities and distances are expressed in radians/sec and radians, and can be easily expressed in meters/sec and meters respectively by multiplying the velocities and distances by the wheel radius (0.31 m).

The nominal μ-λ curve has a maximum μ value of 0.5 and the corresponding λ value of 0.175. The nominal road condition is utilized in designing the active sliding mode

traction controller. Our intent is to simulate performance under wide varying road surface conditions. We chose nominal road condition for the control design purposes such that the μ value would be the average of the values for extreme conditions. The nominal $\mu - \lambda$ curve corresponds to an earth road. However, note that this nominal condition does not reflect the standard highway condition. Simulations are performed on dry concrete road and a slippery road to show extreme road conditions. It is important to analyze the performance in the whole range of road conditions, for the presence of substances like grease and dirt can cause the surface conditions to vary. We have chosen to use the varying surface conditions for evaluating external disturbances, because they have a pronounced effect on the performance of vehicles in terms of their stability. For dry concrete road the maximum μ value of 0.8 is chosen and the corresponding λ is 0.2, whereas, for a slippery road, the maximum μ value of 0.2 is chosen and the corresponding λ is 0.15. The $\mu - \lambda$ relationship is analytically approximated by:

$$\mu = 0.3\, \mu_p \lambda / (\lambda_p^2 + \lambda^2) \tag{72}$$

where μ_p represents the peak μ, and λ_p represents the corresponding wheel slip.

For simulations, Using Table 3, the following parameters are calculated to be

$$b_{1N} = 14.7548$$

$$b_{2N} = 35.2284$$

$$b_3 = 0.0497 \tag{73}$$

Parametric uncertainty is taken to be about 25% for all parameters. The sampling frequency in the simulation is 0.5 kHz.

The simulation results for the slip control (34) for desired slip equal to 0.15 are shown in Figure 8 and Figure 9. Figure 8 shows the simulation performed on a slippery road and Figure 9 shows the simulation performed on dry concrete. Both figures show good wheel slip tracking in spite of 25% modeling errors in the parameters.

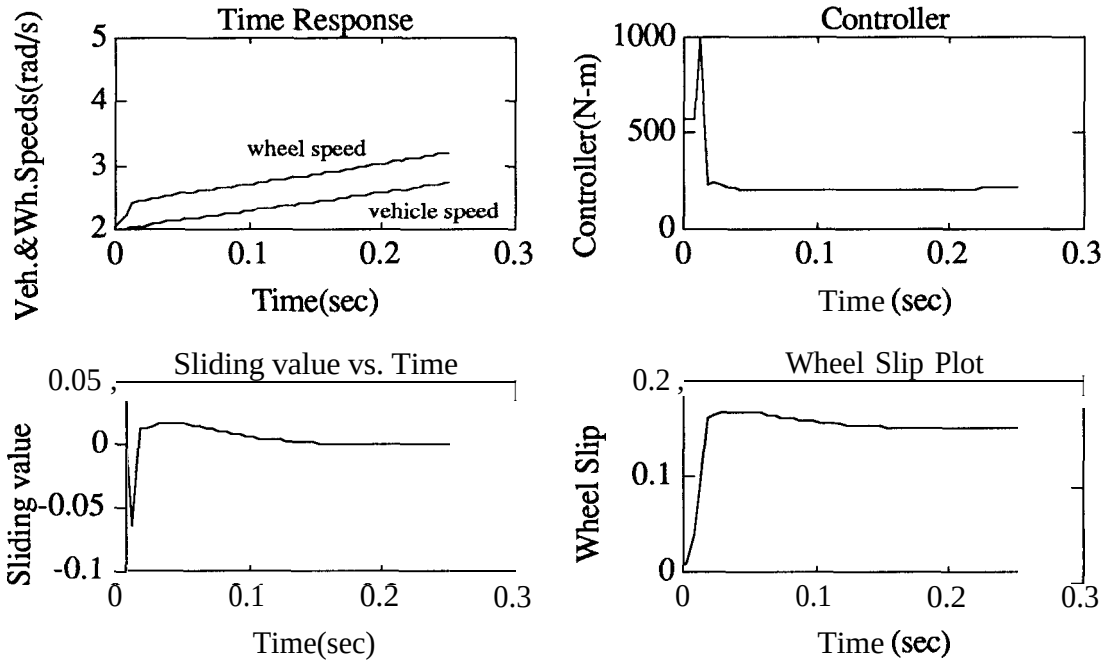

Figure 8 Wheel Slip Control on a Slippery Road

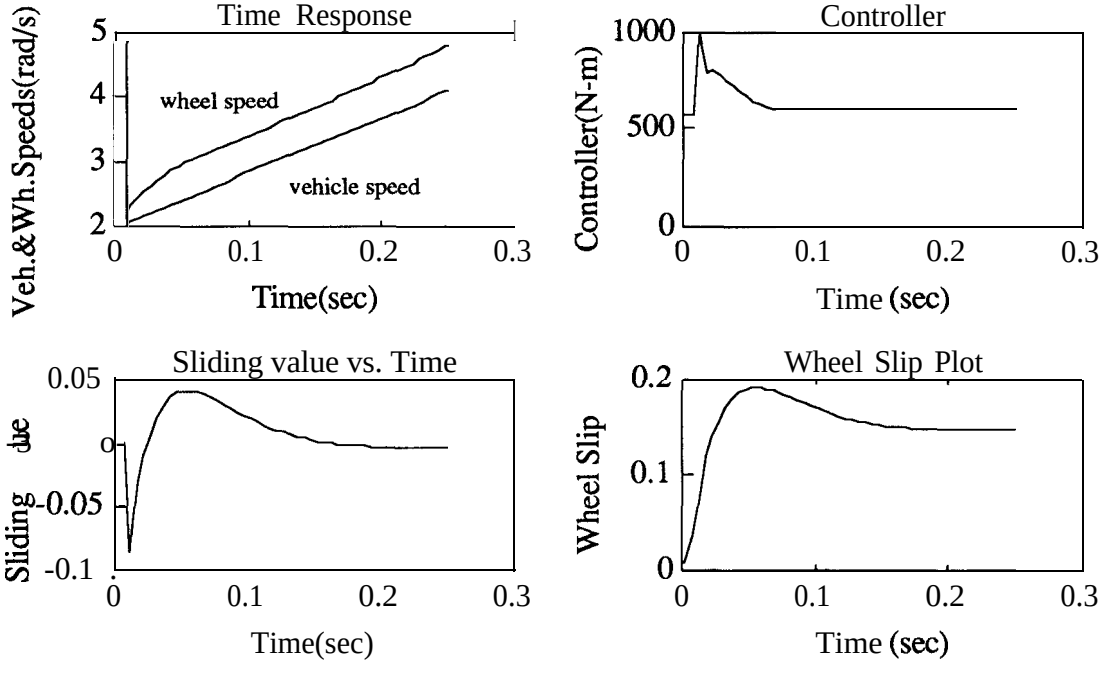

Figure 9 Wheel Slip Control on Dry Concrete

The simulation results for the passive PID control law (65) are shown in Figure 10. From the plot of the results, the performance is satisfactory. The disadvantage of this law is that the gains of the controller have to be tuned based on trial and error, or by ignoring the coupling of the two dynamic equations of the system.

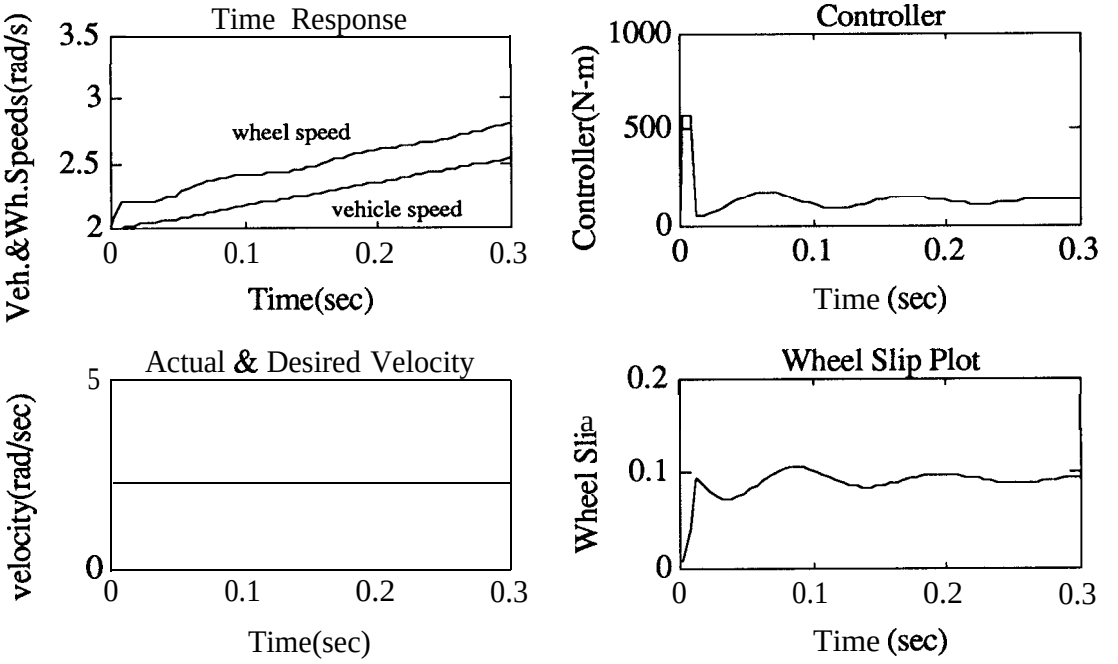

Figure 10 Tractionless PID Control

Simulation results for the longitudinal traction control of a vehicle trying to maintain a constant spacing between itself and a vehicle in front while accelerating, using the two sliding surface method described in section-7, are shown in Figure 11 and Figure 12. Figure 11 shows the simulation on a slippery road, while Figure 12 shows the simulation on dry concrete. The desired adhesion in the longitudinal direction is provided by the first sliding surface, as given by Equation (63). The torque input is computed using Equation (34), where the second sliding surface is defined in Equation (64). The calculation of the desired wheel slip is based on the nominal $\mu-\lambda$ curve. The actual and desired velocities follow each other very closely even in the presence of parametric uncertainties. The spacing errors (not shown in the plots) are however smaller than those obtained by using

the passive PID control law. Notice that wheel slip is higher on the slippery road than on dry concrete.

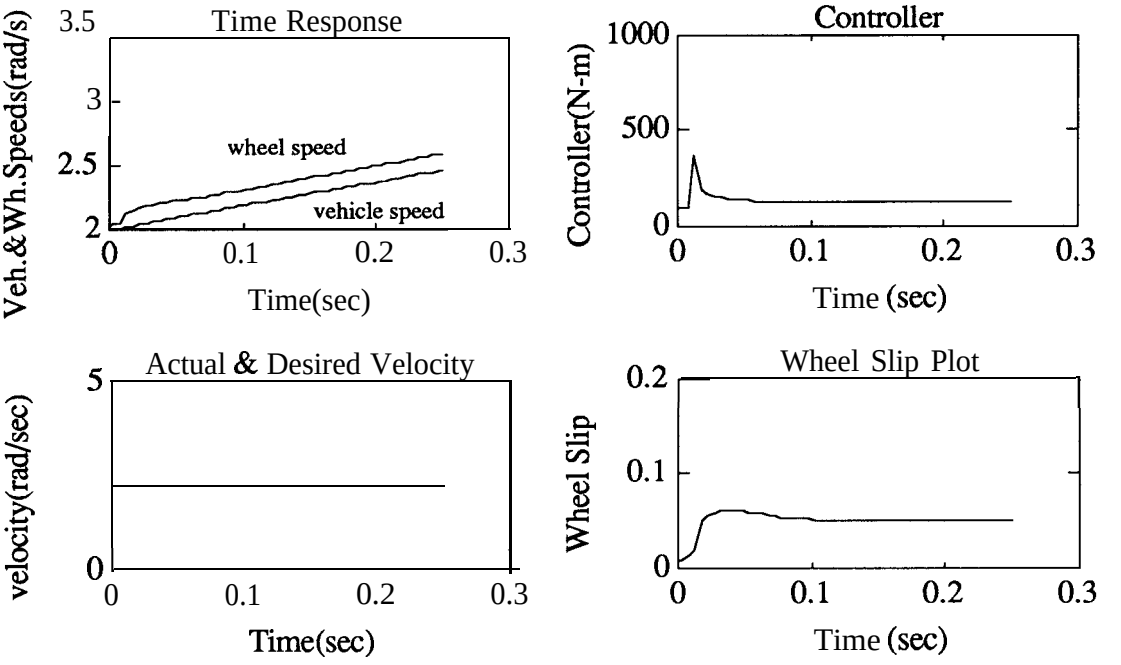

Figure 11 Longitudinal Control with Traction on a Slippery Road

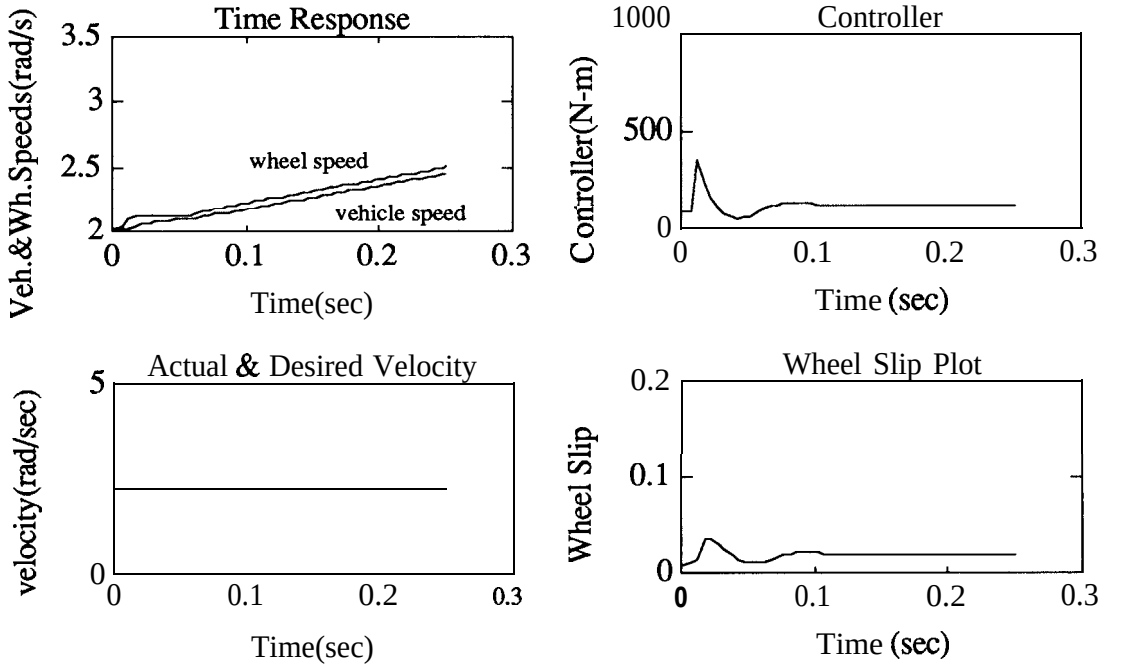

Figure 12 Longitudinal Control with Traction on Dry Concrete

Results of the traction control which was synthesized with the sliding mode estimation scheme for time optimal control while accelerating a vehicle, are shown in Figure 13 and Figure 14. Figure 13 shows the simulation on a slippery road, while Figure 14 shows the simulation on dry concrete. The peak slip for the slippery road is 0.15 and that for dry concrete is .2. The simulation results are satisfactory as the peak slips are followed quite well after brief transients.

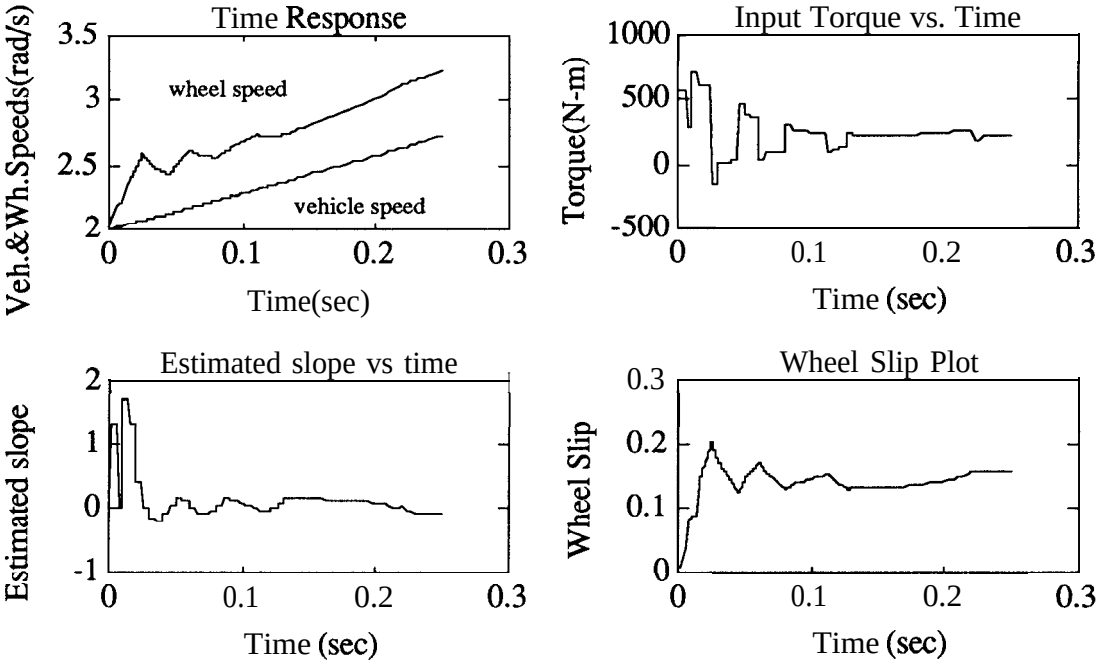

Figure 13 Traction Control for Fastest Acceleration on a Slippery Road

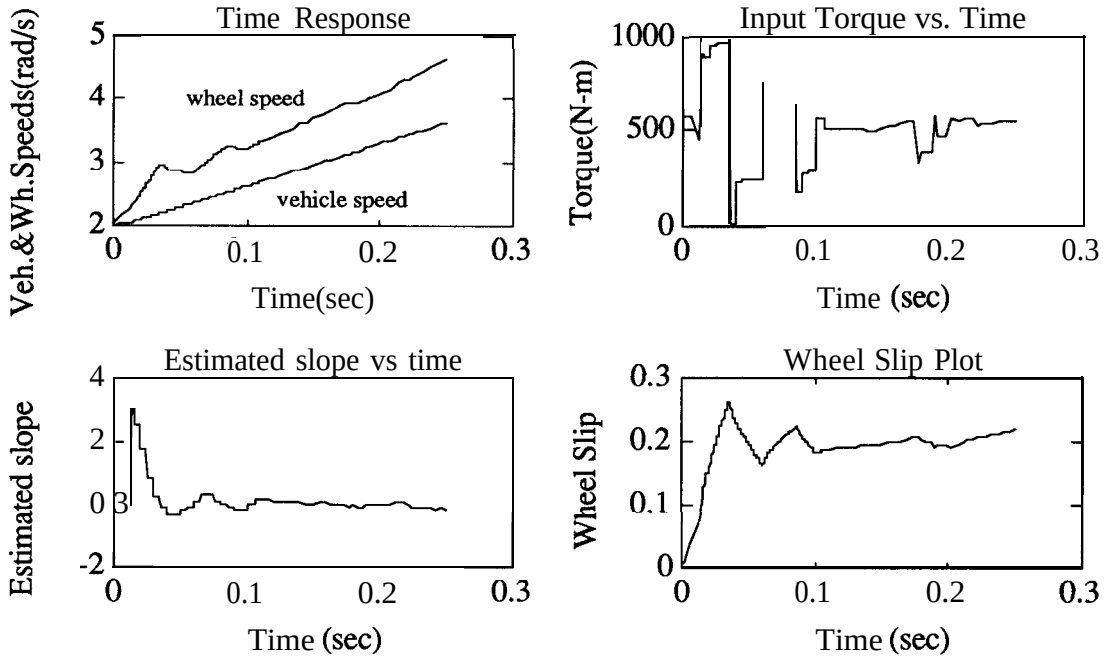

Figure 14 Traction Control for Fastest Acceleration on Dry Concrete

A tractionless single surface sliding mode controller (71) is used for longitudinal control and the results are shown in Figure 15. The tracking is satisfactory.

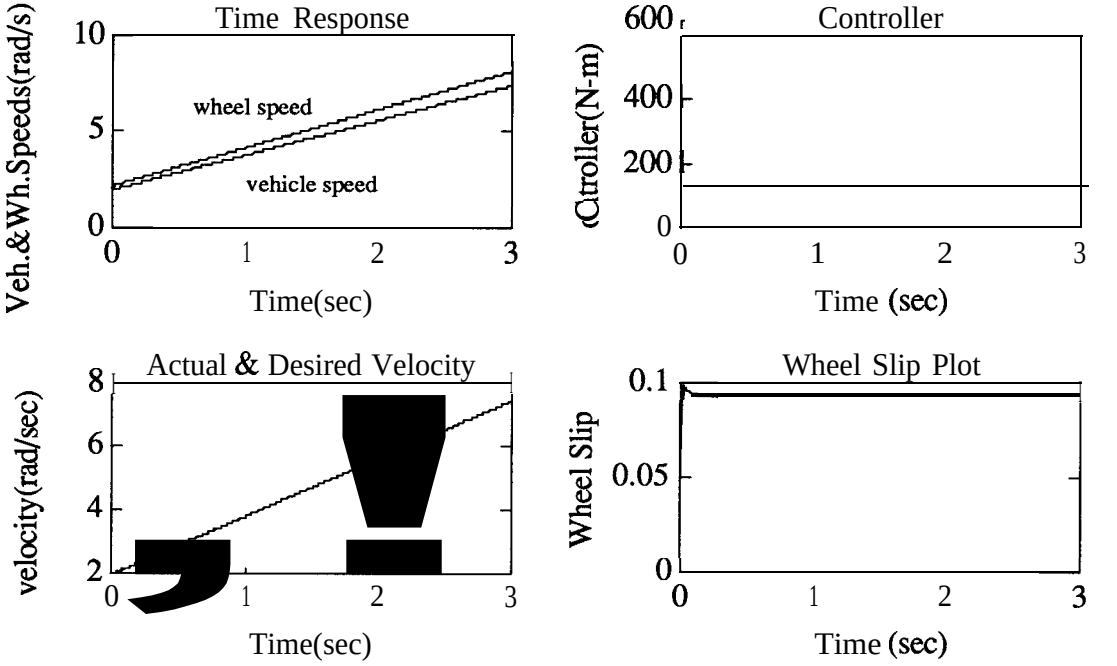

Figure 15 Tractionless Longitudinal Control

Comparison of the robustness of the traction controller with tractionless controllers, to external disturbances on a slippery road, is performed next. The combination of a slippery road condition with a strong wind gust provides a good testing conditions for the robustness comparison. In the longitudinal vehicle tracking while using the sliding mode passive controller, when a wind force disturbance of $0.2g$ (g is the acceleration due to gravity) is given at 0.3 seconds from the start of the simulation, for a period of 0.05 seconds, the slip becomes uncontrollable, as shown by Figure 16. The disturbance forces the slip to attain values greater than 0.15, thereby causing it to be in the negative $\mu - \lambda$ slope region. This makes the system unstable. Similar instability is seen in Figure 17 when the same disturbance is given to the system, which is being controlled by the PID passive control law, at 0.5 seconds from the start. However, using the control law with the traction controller, as illustrated in Figure 18, the system remains stable when it encounters the same disturbance at 0.3 seconds from the start. Although the disturbance used in these simulations is not practical for the actual vehicle system, it gives insight into the stability of the various longitudinal controllers during simulation.

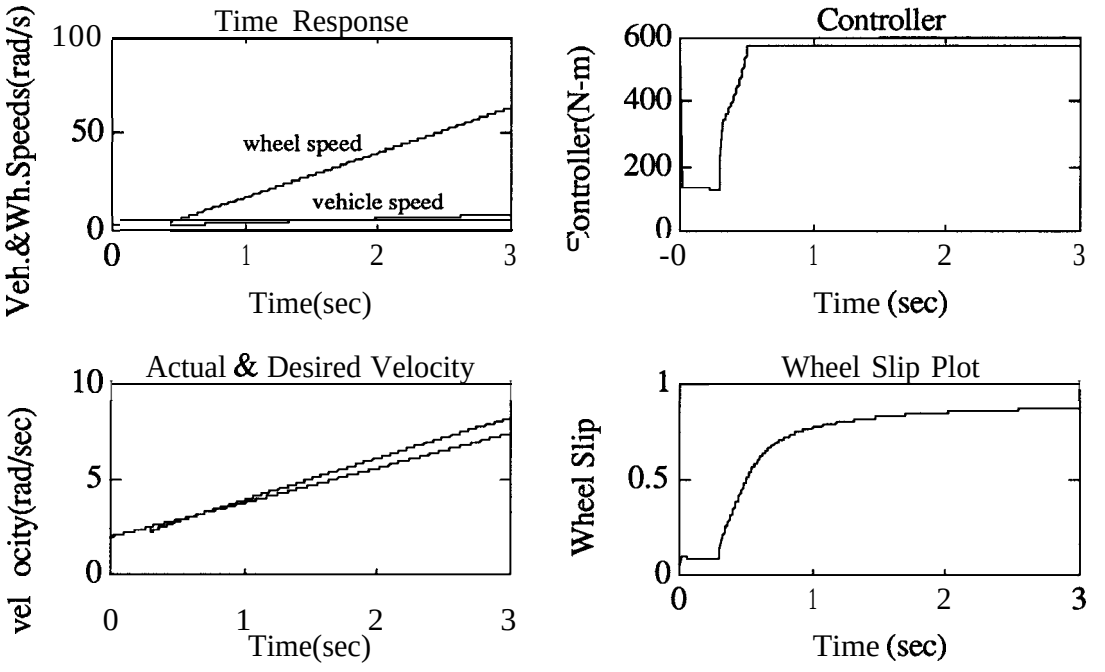

Figure 16 Tractionless Control with Wind Disturbance

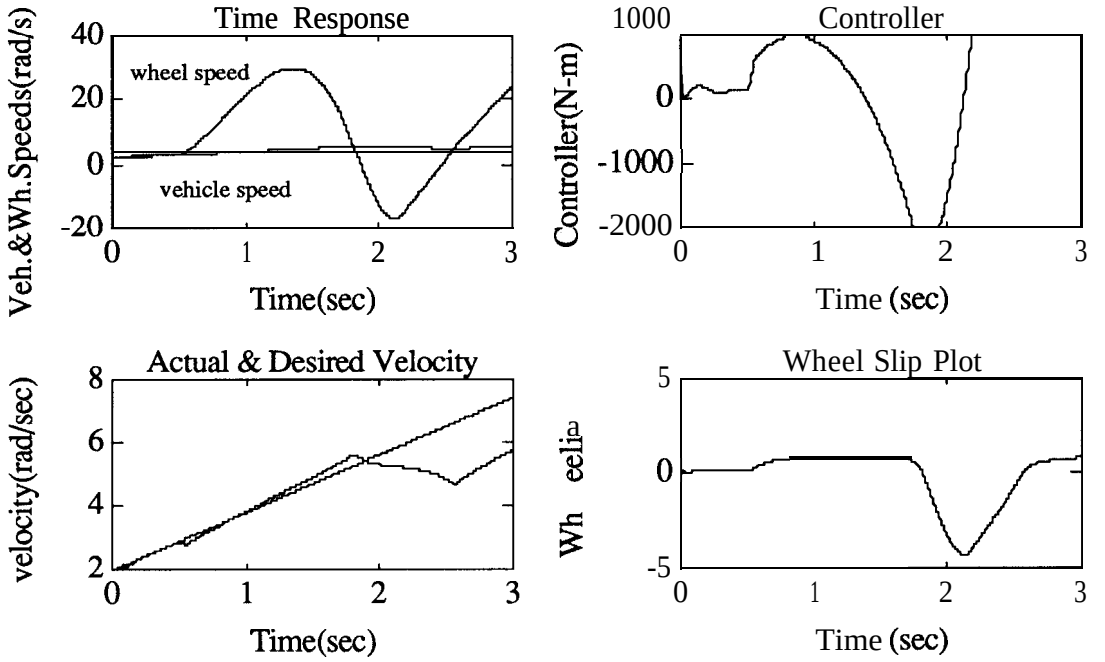

Figure 17 Tractionless PID Control with Wind Disturbance

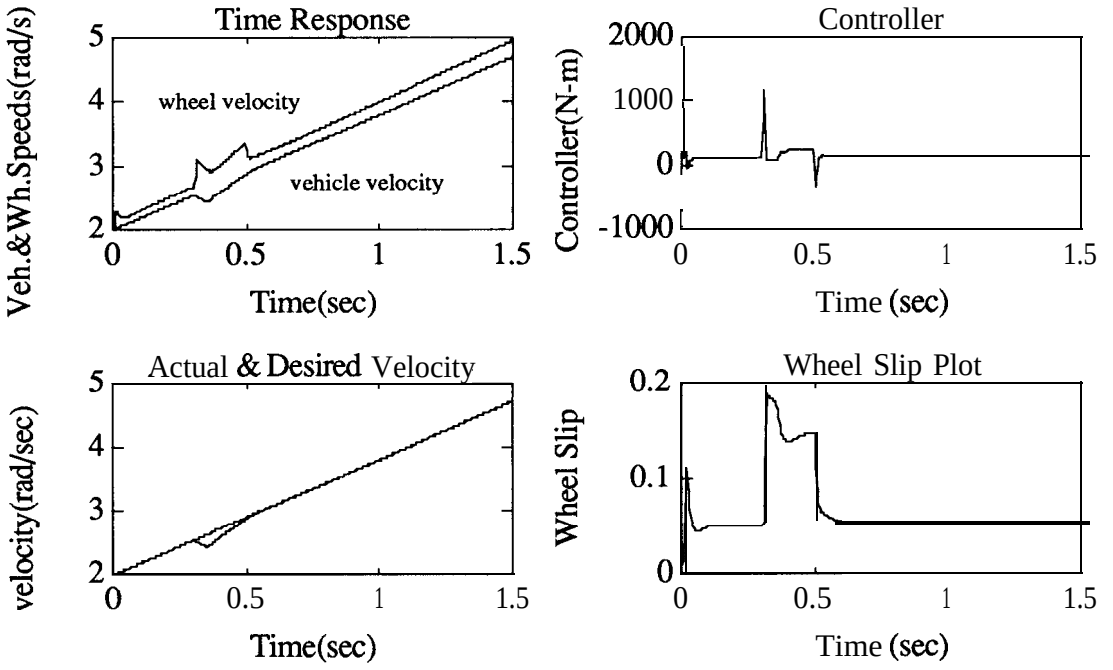

Figure 18 Traction Control with Wind Disturbance

11. Conclusions

It was shown that traction control is important for safety and highway automation of vehicles. A robust control strategy was designed for slip control, which in turn controls the traction. It was shown how traction control can be used to satisfy different objectives of vehicle control. The importance of traction control was further emphasized by comparing its performance to passive controllers in a simulation study in which an impulse-like wind disturbance was introduced. The comparative study showed that the system under traction control is stable in the presence of external disturbances, whereas the system under passive control may become unstable in the presence of external disturbances.

Traction control can be used to enhance the performance of a single independent vehicle with a complete set of sensors and controller integrated in a single system, or a platoon of vehicles, where the sensors and the controllers are distributed within the vehicles and the roadway, It can be used to accelerate or decelerate a single vehicle in the minimum time, or it can be used to enhance the maneuvering ability of a vehicle, especially during severe steering actions. Traction control also improves the performance of platoon of vehicles in terms of stability and achieving a tighter control. Traction control makes the system robust to external disturbances and provides a better control especially during significant lateral maneuvers.

Further study of traction control is in progress including evaluation of traction control as a part of integrated longitudinal and lateral control strategy.

12. Acknowledgments

This work was performed as part of the PATH Program of the University of California, in cooperation with the State of California, Business and Transportation Agency, Department of Transportation, and the United States Department of

Transportation, Federal Highway Administration.

The contents of this report reflect the views of the authors who are responsible for the facts and the accuracy of the data presented herein. The contents do not necessarily reflect the official views or policies of the State of California. This report does not constitute a standard, specification, or regulation.

References

[1] Anderson, B. D. O., and Moore, J. B., ***Optimal Control-Linear Quadratic Methods,*** Englewood Cliffs, NJ: Prentice Hall, 1990.

[2] Birch, S., Vehicle Sensor, ***Automotive Engineering,*** Vol. 97, No. 6, 91-92, June 1989

[3] Gupta, N., Frequency-Shaped Cost Functionals: Extension of Linear-Quadratic-Gaussian Design Method, ***J. Guidance and Contr.,*** vol. 3, no. 6, pp. 529-535, Nov.-Dec. 1980.

[4] Green, J., and Hedrick, J. K., Nonlinear Torque Control for Gasoline Engines, *Proc.* ***ACC,*** 1990.

[5] Harned, J. L., et al., Measurement of Tire Break Force Characteristics as related to Wheel Slip Control System Design, SAE Trans. Vol. 78, pp. 909-925, No. 690214, 1969.

[6] Leiber, H. et al., Anti-Skid System (ABS) for Passenger ***Cars, Bosch Technical and Scientific Report,*** Feb. 1982.

[7] Leiber, H., and Czinczel, A., Four Years of Experience with 4-Wheel Antiskid Brake (ABS), ***SAE*** 830481, 1983.

[8] Peng, H., and Tomizuka, M., Vehicle Lateral Control for Highway Automation, ***ACC Proceedings,*** San Diego., pp. 788-794, 1990.

[9] Matsumoto, N., and Tomizuka, M., Vehicle Lateral Velocity and Yaw Rate Control with Two Independent Control Inputs, ***Trans. of the ASME ,*** 114, pp. 606-613, 1992.

[10] Rohrs, C. E., Valavani, L. S., Athans, M., and Stein, G., Robustness of Continuous-Time Adaptive Control Algorithms in the Presence of Unmodeled Dynamics, ***IEEE Trans. on Aut. Cont., 30,*** pp. 881-889, 1985.

[11] Schurr, H., and Dittner, A., A New Anti-skid-Brake System for Disc and Drum Brakes, Braking: Recent Developments, ***SAE 840486,*** May 1984.

[12] Slotine, J.-J. E., and Coetsee, J. A., Adaptive Sliding Controller Synthesis for Nonlinear Systems, ***Int. J. Control ,*** 1986.

[13] Slotine, J.-J. E., and Li, Weiping, ***Applied Nonlinear Control,*** Prentice Hall, New Jersey, 1991.

[14] Taborek, J. J., ***Mechanics of Vehicle,*** Penton, Cleveland, 1957.

[15] Taheri, S., A Feasibility Study of the Use of a New Nonlinear Control Law for Automobile Anti-lock Braking Systems, ***ACC Proceedings,*** vol. 2 of 3, 1990.

[16] Taheri, S., A, and Law, E. H., Investigation of Integrated Slip Control Braking and Closed Loop Four Wheel Steering Systems for Automobiles during Combined Hard Braking and Severe Steering, ***ACC Proceedings,*** vol.2, 1990.

[17] Tan, H. S., Adaptive and Robust Controls with Application to Vehicle Traction Control, ***Ph.D. Dissertation,*** University of California, Berkeley, 1988.

[18] Tan, H. S., and Tomizuka, M., A Discrete-Time Robust Vehicle Traction Controller Design, ***ACC Proceedings,*** pp. 1053-1058, 1989.

[19] Tan, H. S., and Tomizuka, M., An Adaptive Sliding Mode Vehicle Traction Controller Design, ***ACC Proceedings,*** vol. 2 of 3, pp. 1856-1861, 1990.

[20] Wong, J. ***Y., Theory of Ground Vehicles,*** Wiley, New York,, 1978.